PROCEEDINGS A

royalsocietypublishing.org/journal/rspa

Research

Cite this article: Adhikari S. 2021 The eigenbuckling analysis of hexagonal lattices: closed-form solutions. *Proc. R. Soc. A* **477**: 20210244.
https://doi.org/10.1098/rspa.2021.0244

Received: 15 March 2021
Accepted: 10 June 2021

Subject Areas:
mechanical engineering, structural engineering

Keywords:
elastic buckling, lattice materials, Euler–Bernoulli beams, effective elastic moduli, nonlinear stress–strain

Author for correspondence:
S. Adhikari
e-mail: S.Adhikari@swansea.ac.uk

Electronic supplementary material is available online at rs.figshare.com.

THE ROYAL SOCIETY PUBLISHING

The eigenbuckling analysis of hexagonal lattices: closed-form solutions

S. Adhikari

College of Engineering, Swansea University, Bay Campus, Fabian Way, Crymlyn Burrows, Swansea SA1 8EN, UK

SA, 0000-0003-4181-3457

Elastic instability such as the buckling of cellular materials plays a pivotal role in their analysis and design. Despite extensive research, the quantification of critical stresses leading to elastic instabilities remains challenging due to the inherent nonlinearities. We develop an analytical approach considering the spectral decomposition of the elasticity matrix of two-dimensional hexagonal lattice materials. The necessary and sufficient condition for the buckling is established through the zeros of the eigenvalues of the elasticity matrix. Through the analytical solution of the eigenvalues, the conditions involving equivalent elastic properties of the lattice were directly connected to the mathematical requirement of buckling. The equivalent elastic properties are expressed in closed form using geometric properties of the lattice and trigonometric functions of a non-dimensional axial force parameter. The axial force parameter was identified for four different stress cases, namely, compressive stress in the longitudinal and transverse directions separately and together and torsional stress. By solving the resulting nonlinear equations, we derive exact analytical expressions of critical eigenbuckling stresses for these four cases. Crucial parameter combinations leading to minimum buckling stresses are derived analytically. The exact closed-form analytical expressions derived in the paper can be used for quick engineering design calculations and benchmarking related experimental and numerical studies.

1. Introduction

Cellular solids are a class of mechanical metamaterials [1] which can be designed to possess extraordinary properties not found in natural materials. Such properties include but are not limited to excellent strength to

weight ratio [2,3], outstanding energy absorption and impact resistance and non-reciprocal response [4]. We refer to the book by Gibson & Ashby [5] and a recent review paper [6] for a general introduction to cellular solids and an overview of analytical methods and experimental results in the field. Hexagonal lattices, also known as honeycombs, are a special class of two-dimensional (2D) lattices that are common across a wide range of engineering application areas. The mechanics of hexagonal lattices plays a key role in understanding nanoscale material systems such as single-layer graphene [7], boron nitride nanosheets [8] and multilayer nano-heterostructures [9]. Recent developments in additive layer manufacturing (3D printing) and multiphysics applications involving electromechanical and piezoelectric phenomena [10] demands an advanced understanding of cellular materials than ever before.

Cellular materials are made of periodic unit cells. When the number of cells is sufficiently large, cellular materials can be effectively modelled as a continuum with equivalent elastic properties [11]. Such equivalent proprieties can be derived from the mechanics of a unit cell. This approach is not only computationally efficient but also physically insightful [12,13]. When the cellular material is not perfectly periodic, a representative unit cell approach was recently developed [14] to generalize the classical unit cell formulation to obtain equivalent elastic moduli. While these unit cell-based methods can be efficient in obtaining overall linear elastic properties, the analysis of buckling and other instabilities is more challenging due to the need to consider inherent non-linearities. Experimental and analytical approaches for a comprehensive understanding of and buckling behaviour of honeycombs were developed in [15]. An instability analysis of metallic hexagonal lattices under general in-plane loads was conducted using theoretical approaches in [16]. On the other hand, Klintworth & Stronge [17] considered transverse loading for theoretical analysis of elastoplastic yielding and cursing. Since these earlier works, many authors (see for example [18–24]) have considered numerical, theoretical and experimental studies on crushing, buckling, instability analysis and general response characterization of cellular materials under compressive loading. Several novel analytical methods for uniaxial buckling analysis were proposed by Fan *et al.* [25] for different periodic lattices. Che & Pugno [26] considered the in-plane buckling of hierarchical honeycomb materials. Haghpana *et al.* [27] developed structural mechanics-based analytical methods for buckling analysis of different lattices.

From this brief literature review, it is evident that extensive research has been conducted on the buckling of lattice materials. Computational and experimental works have provided an excellent physical understanding of the mechanisms underpinning such behaviour. However, a direct and simple analytical quantification of the external stresses which will initiate buckling in a general lattice structure has remained an open problem. Very accurate and experimentally validated empirical formulae (see for example [5]) are available for different loading cases for both two- and three-dimensional lattices with a range of geometrical shapes. This paper aims to adopt a physics-based analytical approach as opposed to an empirical one. The key advantage of such an approach is that the parametric dependence of the buckling stress will be explicitly known. The majority of physics-based approaches consider a structural mechanics perspective for a representative unit cell. Here, we consider a 'materials' perspective based on the equivalent homogeneous properties of the 2D lattice material. The equivalent elastic properties are obtained from the mechanics of a beam-based unit cell. Although geometric nonlinearities are considered in an exact manner by solving the governing ordinary differential equation, linear material behaviour is assumed. Once the elasticity tensor of the 2D continuum material is known, the attention is focused on the spectral decomposition [28,29] of the elasticity matrix. This is in general a complex symmetric matrix with distinct eigenvalues. It is proved that the condition of buckling arises from the zeros of the eigenvalues of this matrix. The eigenvalues are obtained explicitly in closed form, which in turn is used to obtain stresses leading to eigenbuckling of the hexagonal lattice.

The elements of the lattice structure are composed of beams undergoing axial and bending deformations. Using the mechanics of beams with axial forces, the equivalent elastic properties are obtained in the electronic supplementary material. In §2, the general elasticity matrix of 2D orthotropic materials and explicit expressions of the homogeneous elastic properties which form this matrix are given. The analysis of eigenbuckling is carried out in §3 using the spectral

decomposition of the elasticity matrix. In §4, eigenbuckling arising due to a compressive stress only along the longitudinal direction is considered. Eigenbuckling analysis due to a compressive stress only along the transverse direction is discussed in §5. The case when compressive stresses along with both directions are applied is investigated in §6. In §7, eigenbuckling of the lattice is investigated due to an applied torsional stress. New closed-form analytical expressions for critical eigenbuckling stresses are derived for all four cases. Illustrative diagrams are used to explain the results. The condition for minimum critical eigenbuckling stress has been derived for all the three loading conditions. Finally, the main conclusions arising from the paper are drawn in §8.

2. The elasticity tensor of 2D lattice materials

The equivalent elastic properties of a lattice material are fundamental for the global stress–strain analysis. With the equivalent elastic properties, any lattice material, which is discrete in nature, can be treated as a continuum material [11]. This in turn allows one to employ analytical and design methods historically developed for complex systems made of continuum materials to lattice materials. When in-plane elasticity of 2D continuum materials are considered, the constitutive relationship can be expressed as

$$\begin{Bmatrix} \varepsilon_{11} \\ \varepsilon_{22} \\ 2\varepsilon_{12} \end{Bmatrix} = \begin{bmatrix} \dfrac{1}{E_1} & -\nu_{21}/E_2 & 0 \\ -\nu_{12}/E_1 & \dfrac{1}{E_2} & 0 \\ 0 & 0 & \dfrac{1}{G_{12}} \end{bmatrix} \begin{Bmatrix} \sigma_{11} \\ \sigma_{22} \\ \sigma_{12} \end{Bmatrix}. \tag{2.1}$$

This is based on the fact that the material is orthotropic [30]. Here, $\varepsilon_{(\bullet)}$ and $\sigma_{(\bullet)}$ represent strain and stress within the 2D material. In the above equation, E_1 is the longitudinal Young's modulus, E_2 is the transverse Young's modulus, G_{12} is the shear modulus, ν_{12} and ν_{21} are the Poisson's ratios. These five quantities explicitly define the stress–strain relationship. This can be illustrated by inverting the coefficient matrix in equation (2.1) as

$$\underbrace{\begin{Bmatrix} \sigma_{11} \\ \sigma_{22} \\ \sigma_{12} \end{Bmatrix}}_{\boldsymbol{\sigma}} = \underbrace{\begin{bmatrix} \dfrac{E_1}{(1-\nu_{12}\nu_{21})} & \dfrac{\nu_{21}E_1}{(1-\nu_{12}\nu_{21})} & 0 \\ \dfrac{\nu_{12}E_2}{(1-\nu_{12}\nu_{21})} & \dfrac{E_2}{(1-\nu_{12}\nu_{21})} & 0 \\ 0 & 0 & G_{12} \end{bmatrix}}_{\mathbf{D}} \underbrace{\begin{Bmatrix} \varepsilon_{11} \\ \varepsilon_{22} \\ 2\varepsilon_{12} \end{Bmatrix}}_{\boldsymbol{\varepsilon}} \tag{2.2}$$

or in the matrix form as

$$\boldsymbol{\sigma} = \mathbf{D}\boldsymbol{\varepsilon}. \tag{2.3}$$

For equation (2.2) to be valid, it is required that $\nu_{12}\nu_{21} \neq 1$, a condition likely to be met by most orthotropic materials. In the above equation, the 3×3 matrix $\mathbf{D}$ is the elasticity matrix for two-dimensional materials. This is not specific to the lattice materials. However, for the lattice materials, the elements of the $\mathbf{D}$ matrix can be explicitly expressed in terms of micro-structural geometric and material properties.

The equivalent elastic properties of a lattice material can be obtained by making use of the periodicity of a suitably selected unit cell. In figure 1, we show a representative example of a hexagonal lattice and its corresponding unit cell. The unit cell is selected such that it represents the whole lattice under tessellation in both directions. Each of the cell walls will bend and compress when subjected to in-plane compressive stress. When the applied stress is uniform along the out-of-plane direction, each element of the unit cell in figure 1*b* can be modelled as a beam. A key focus of this paper is to explicitly consider in-plane compressive stress and understand the buckling behaviour of 2D lattices. In general, a nonlinear stress–strain relationship is expected. This, in turn, will be reflected in the elastic constants which are depended on the applied stress. When external compressive stress is applied to a cellular material as depicted in

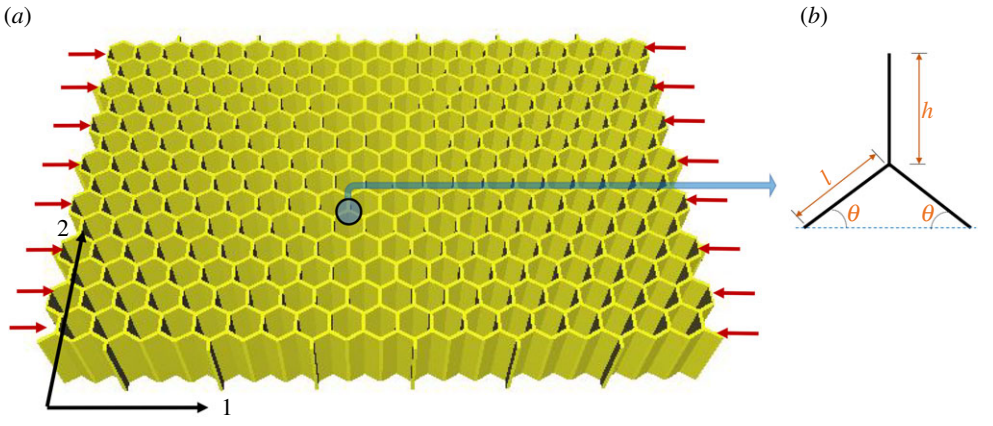

Figure 1. (*a*) Illustration of a hexagonal lattice subjected to compressive stress in direction 1. (*b*) The unit cell is used to analyse the mechanics of the lattice. It comprises three beams connected at one point. The length of the inclined beams is *l* and the length of the vertical beam is *h*. The cell angle is denoted by θ. The thickness of all the beams is *t*. (Online version in colour.)

figure 1*a*, it results in forces and moments on the unit cell shown in figure 1*b*. The deformation of the unit cell due to the applied compressive stress can be obtained using the coefficients of the stiffness matrix of the beam elements. The exact stiffness matrix of beams subjected to axial force can be analytically obtained by solving the underlying fourth-order differential equation with appropriate boundary conditions. Following the analytical derivation illustrated in the electronic supplementary material, the exact expressions of the five elastic constants are given by the following concise closed-form expressions:

$$E_1 = \frac{E\alpha^3 d_1 \cos\theta}{(\beta + \sin\theta)\left(12\sin^2\theta + d_1\alpha^2\cos^2\theta\right)}, \tag{2.4}$$

$$E_2 = \frac{E\alpha^3 d_1(\beta + \sin\theta)}{(12 - d_1\alpha^2)\cos^3\theta + d_1\alpha^2(2\beta + 1)\cos\theta}, \tag{2.5}$$

$$\nu_{12} = \frac{\cos^2\theta\,(12 - d_1\alpha^2)}{(\beta + \sin\theta)\sin\theta\,(12 + d_1\alpha^2\cot^2\theta)}, \tag{2.6}$$

$$\nu_{21} = \frac{(\beta + \sin\theta)\sin\theta\,(12 - d_1\alpha^2)}{(12 - d_1\alpha^2)\cos^2\theta + d_1\alpha^2(2\beta + 1)} \tag{2.7}$$

and

$$G_{12} = \frac{E\alpha^3(\beta + \sin\theta)}{\left(\beta^2(6/d_2 + 2\beta) + \alpha^2\left(\cos\theta + (\beta + \sin\theta)\tan\theta\right)^2\right)\cos\theta}. \tag{2.8}$$

In the above equations, E is the elastic modulus of the base material, θ is the cell angle as shown in figure 1*b*, α and β are geometric non-dimensional ratios given by

$$\alpha = \frac{t}{l}\ \text{(thickness ratio)} \quad \text{and} \quad \beta = \frac{h}{l}\ \text{(height ratio)}. \tag{2.9}$$

The coefficients d_1 and d_2 are functions of a non-dimensional external compressive stress parameter μ expressed by

$$\mu^2 = \frac{Nl^2}{EI}. \tag{2.10}$$

Here, N is in the compressive axial force within the beam (to be determined later in the paper based on applied external stresses) and EI is the bending rigidity. Following the details given in the electronic supplementary material, the exact closed-form expressions of coefficients d_1 and d_2

appearing in the expression of the equivalent elastic properties are given by

$$\left.\begin{aligned} d_1 &= -\frac{\mu^3 \sin(\mu)}{\Delta}, d_2 = \frac{\mu^2(\cos(\mu)-1)}{\Delta} \\ \text{and} \qquad \Delta &= \mu \sin(\mu) - 2(1-\cos(\mu)). \end{aligned}\right\} \tag{2.11}$$

Note that the coefficients d_1 and d_2 are nonlinear functions of the axial force parameter μ. Consequently, the equivalent elastic properties also become nonlinear functions of μ.

3. The analysis of eigenbuckling of lattice materials

We take a 'materials' point of view for the buckling analysis of 2D lattices. In a recent paper [31], the elements of the elasticity matrix $\mathbf{D}$ in equation (2.2) were derived using dynamic considerations. Owing to the presence of damping, it was shown that the elements of the $\mathbf{D}$ are complex valued. It turns out that $\mathbf{D}$ is a complex symmetric matrix (not Hermitian). The symmetry of the matrix $\mathbf{D}$ arises from the fact that $\nu_{21}E_1 = \nu_{11}E_2$. Although the $\mathbf{D}$ matrix is real in this paper, for analysis of eigenbuckling, we will consider it to be complex for generality. The approach adopted here is based on the spectral decomposition of the elasticity tensor [28,29]. One of our main propositions regarding the eigenbuckling of 2D lattice materials is the following.

Lemma 3.1. *The necessary and sufficient condition for buckling is that at least one eigenvalue of the elasticity matrix $\boldsymbol{D}$ is zero.*

Proof. We first consider the complex-valued eigenvalue problem involving the symmetric elasticity matrix $\mathbf{D} \in \mathbb{C}^{3\times 3}$ as

$$\mathbf{D}\boldsymbol{\phi}_j = \lambda_j \boldsymbol{\phi}_j, \quad j = 1,2,3. \tag{3.1}$$

Using the eigenvalues λ_j and the eigenvectors $\boldsymbol{\phi}_j$, the following matrices are created

$$\boldsymbol{\Lambda} = \operatorname{diag}[\lambda_1, \lambda_2, \lambda_3] \in \mathbb{C}^{3\times 3} \quad \text{and} \quad \boldsymbol{\Phi} = \left[\boldsymbol{\phi}_1, \boldsymbol{\phi}_2, \boldsymbol{\phi}_3\right] \in \mathbb{C}^{3\times 3}. \tag{3.2}$$

For orthotropic materials, the eigenvalues will be distinct. Therefore, utilizing the similarity transformation [32], one has

$$\boldsymbol{\Phi}^{-1}\mathbf{D}\boldsymbol{\Phi} = \boldsymbol{\Lambda} \quad \text{or } \mathbf{D}^{-1} = \boldsymbol{\Phi}\boldsymbol{\Lambda}^{-1}\boldsymbol{\Phi}^{-1}. \tag{3.3}$$

Using this, from equation (2.3), we can obtain the stain in terms of the eigensolutions as

$$\boldsymbol{\varepsilon} = \mathbf{D}^{-1}\boldsymbol{\sigma} = \left[\boldsymbol{\Phi}\boldsymbol{\Lambda}^{-1}\boldsymbol{\Phi}^{-1}\right]\boldsymbol{\sigma}. \tag{3.4}$$

At the onset of buckling, an infinite stain will occur due to finite stress. Since the modal matrix, $\boldsymbol{\Phi}$ is invertible as the eigenvalues are distinct, the only way the elements of the strain vector $\boldsymbol{\varepsilon}$ can be infinite is if one of the eigenvalues in the $\boldsymbol{\Lambda}$ matrix is zero. This proves the sufficient condition.

To prove the necessary condition, consider that all eigenvalues are non-zero, that is $\lambda_j \neq 0, j = 1,2,3$. Then, $\boldsymbol{\Lambda}^{-1}$ will be finite and from equation (3.4), we obtain that $\boldsymbol{\varepsilon}$ will be finite if $\boldsymbol{\sigma}$ is finite. This does not satisfy the condition of buckling, that is the strain must be infinite. This completes the proof. ∎

Although the condition of buckling given in lemma 3.1 is in terms of the eigenvalues of the elasticity matrix $\mathbf{D}$, it is not directly useful unless the eigenvalues are available. The eigenvalue problem involving the elasticity matrix $\mathbf{D}$ can be expressed as

$$\det(\mathbf{D} - \lambda\mathbf{I}) = 0. \tag{3.5}$$

The characteristic equation arising from the above determinant can be simplified as

$$\lambda^3 + \underbrace{\frac{(-G_{12}\nu_{12}b + E_1 + E_2 + G_{12})\,\lambda^2}{\nu_{12}\nu_{21} - 1}}_{a_2} - \underbrace{\frac{(E_2E_1 + E_1G_{12} + E_2G_{12})\,\lambda}{\nu_{12}\nu_{21} - 1}}_{a_1} + \underbrace{\frac{G_{12}E_2E_1}{\nu_{12}\nu_{21} - 1}}_{a_0} = 0. \tag{3.6}$$

Here, a_j is the coefficient associated with $\lambda^j, j = 0, 1, 2$. This is a cubic polynomial, and it can be solved exactly in closed form using Cardano's formula (see for example §3.8 [33]). The three roots are expressed as

$$\lambda_{1,2} = -\frac{a_2}{3} - \frac{1}{2}(S+T) \pm \mathrm{i}\frac{\sqrt{3}}{2}(S-T) \tag{3.7}$$

and

$$\lambda_3 = -\frac{a_2}{3} + (S+T). \tag{3.8}$$

In the above equation

$$S = \sqrt[3]{R+\sqrt{D}}, \quad T = \sqrt[3]{R-\sqrt{D}}, \; D = Q^3 + R^2 \tag{3.9}$$

and

$$Q = \frac{3a_1 - a_2^2}{9} \quad \text{and } R = \frac{9a_2a_1 - 27a_0 - 2a_2^3}{54}. \tag{3.10}$$

After considerable algebraic simplifications, the three roots can be expressed concisely as

$$\left.\begin{aligned} \lambda_{1,2} &= \frac{(E_1+E_2) \pm \sqrt{{E_1}^2 + (4\nu_{12}\nu_{21} - 2)\, E_2E_1 + {E_2}^2}}{2\,(1-\nu_{12}\nu_{21})} \\ \text{and} \qquad \lambda_3 &= G_{12}. \end{aligned}\right\} \tag{3.11}$$

The roots are, in general, complex when the elastic constants are complex valued. If all the elastic constants are real-valued, then all the roots will be real-valued. Considering the case $\lambda_3 = 0$, the required condition for buckling is obtained as

$$G_{12} = 0. \tag{3.12}$$

This implies that if the shear modulus becomes zero, the lattice material will buckle. This is intuitive as for a cellular solid with zero shear modulus means that it behaves like a fluid and hence unstable. There are certain metamaterials, such as the pentamode [34] material, which shows extremely low shear modulus. This may be also realized in other lattices by the application of suitable shear stress and considering geometric nonlinearities. As the main interest in this work is in-plane axial buckling, considering the case $\lambda_{1,2} = 0$, from equation (3.11), one can deduce

$$\begin{aligned} &\frac{(E_1+E_2) \pm \sqrt{{E_1}^2 + (4\nu_{12}\nu_{21} - 2)\, E_2E_1 + {E_2}^2}}{2\,(1-\nu_{12}\nu_{21})} = 0 \\ \text{or } &(E_1+E_2)^2 = {E_1}^2 + (4\nu_{12}\nu_{21} - 2)\, E_2E_1 + {E_2}^2. \end{aligned} \tag{3.13}$$

This can be simplified to obtain the required condition for buckling as

$$4E_2E_1\,(1-\nu_{12}\nu_{21}) = 0. \tag{3.14}$$

It has been established that $\nu_{12}\nu_{21} \neq 1$. Therefore, the condition for buckling can be expressed as

$$E_1 = 0 \quad \text{or } E_2 = 0. \tag{3.15}$$

This result is general and intuitively appealing. However, the derivation itself does not give any clue as to how, or if, this condition will be met for a real lattice material. This is addressed next.

The expressions of E_1 and E_2 when the lattice is subjected to compressive stress is given by equations (2.4) and (2.5). Discarding the degenerate case of $\theta = \pi/2$, the conditions in

equation (3.15) translates to

$$d_1 = 0 \quad \text{or} \quad -\frac{\mu^3 \sin(\mu)}{\Delta} = 0. \tag{3.16}$$

This is a nonlinear equation in μ. As $\Delta \neq 0$, for non-trivial solutions, this requirement results

$$\sin(\mu) = 0 \quad \text{or } \mu^2 = n^2\pi^2, \quad n = 1, 2, 3, \ldots . \tag{3.17}$$

This is the condition of eigenbuckling of 2D lattice materials. The expression of μ is given in equation (2.10). Equation (3.17) does not give the actual force/stress necessary to induce buckling. It only gives the force multiplier. This needs to be used with the actual stress condition applied to the lattice material. The axial force N appearing in the definition of μ in equation (2.10) can be related to various applied stress conditions. In the next sections, four physically realistic cases are considered, namely, stress only along direction 1 (longitudinal direction), stress only along direction 2 (transverse direction), simultaneous stresses along with both directions and shear stress.

4. Eigenbuckling in the longitudinal direction

In figure 2, we show the hexagonal lattice subjected to compressive stress in the longitudinal direction. In the same figure, forcing on the unit cell due to this applied stress is also shown. It can be observed that the compressive axial force in the inclined beam is $N = P\cos\theta$ where

$$P = \sigma_1 b(h + l\sin\theta). \tag{4.1}$$

Here, σ_1 is the applied stress and b is the out-of-plane thickness of the lattice. Using these, the non-dimensional axial force appearing in equation (2.10) can obtained as

$$\begin{aligned} \mu^2 &= \frac{Nl^2}{EI} = \frac{\sigma_1 b(h + l\sin\theta)\cos\theta l^2}{Ebt^3/12} = \left(\frac{\sigma_1}{E\alpha^3}\right) 12(\beta + \sin\theta)\cos\theta \\ \text{or } \mu &= \sqrt{\left(\frac{\sigma_1}{E\alpha^3}\right) 12(\beta + \sin\theta)\cos\theta}. \end{aligned} \tag{4.2}$$

Substituting d_1 from equation (2.11) in equation (2.4), we can express the Young's modulus explicitly in terms of the above non-dimensional axial force parameter as

$$E_1 = \frac{E\alpha^3\mu^3 \sin(\mu)\cos\theta}{(\beta + \sin\theta)\left(\mu^3 \sin(\mu)\alpha^2 \cos^2\theta - 12\sin^2\theta\Delta\right)}. \tag{4.3}$$

This is the explicit expression of the equivalent elastic modulus E_1 of hexagonal lattices subjected to compressive stress as in figure 2.

The substitution of μ from equation (4.2) in the expression of E_1 in equation (4.3) clearly demonstrates that the Young's modulus E_1 is depended on the applied stress σ_1. This is a nonlinear behaviour. The ratio $\sigma_1/E\alpha^3$ is a non-dimensional quantity quantifying the applied compressive stress in direction 1 relative to Young's modulus of the constitutive material. In figure 3, we show the variation of the effective Young's modulus E_1 with respect to this relative compressive stress. The y-axis is normalized with $E\alpha^3$ as the x-axis. Results for four values of the cell angle θ are shown and the height ratio is assumed to be $\beta = h/l = 1$. The thickness ratio is considered to be $\alpha = t/l = 0.1$. As the applied compressive stress increases, the effective Young's modulus E_1 reduces. This is expected because the axial compression results in a loss of stiffness in the constituent beams.

When $E_1 > 0$ in figure 3, the lattice is 'stable' in the sense that it is able to withstand the applied stress and yields a finite strain. The lattice is 'unstable' when $E_1 \leq 0$ and the corresponding zone is marked in the figure. The critical value of the buckling stress is obtained when E_1 makes a transition from a positive to a negative value. When $E_1 = 0$, theoretically the lattice has infinite strain due to a finite stress. This is exactly what is obtained from the eigenbuckling analysis in the

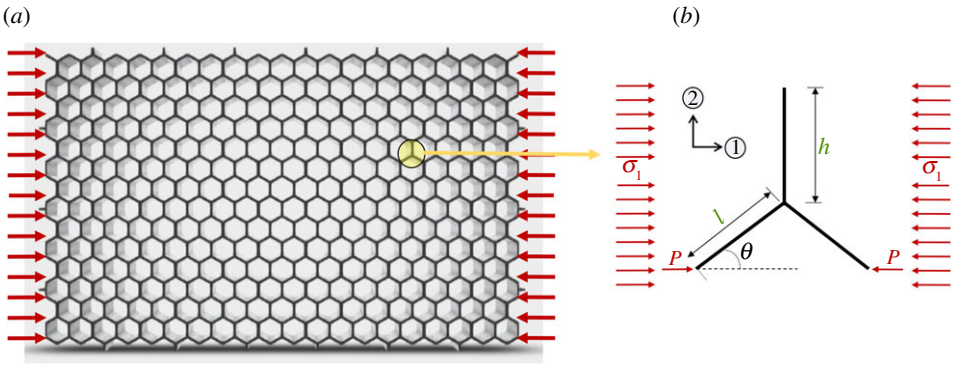

Figure 2. (*a*) Hexagonal lattice subjected to compressive stress σ_1 in the 1-direction (longitudinal direction). (*b*) Forcing in the constituent beams within the unit cell model. The compressive axial force is: $P\cos\theta$ with $P = \sigma_1 b(h + l\sin\theta)$, where b is the out-of-plane thickness of the lattice. (Online version in colour.)

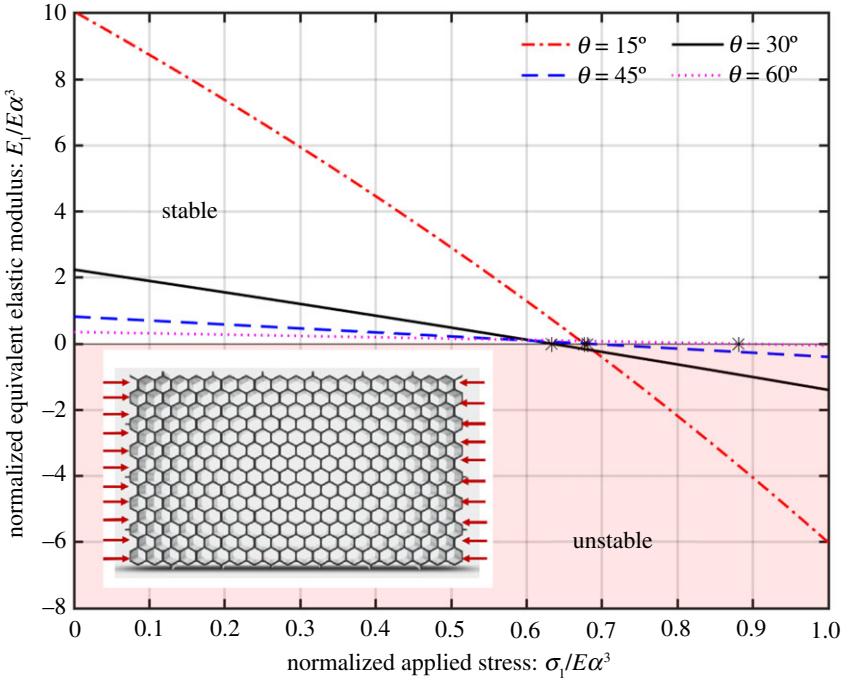

Figure 3. Variation of the effective Young's modulus E_1 with respect to the relative compressive stress in the 1-direction. The horizontal and vertical axis are normalized at $E\alpha^3$. Results for four values of the cell angle θ are shown. The values of the height ratio and the thickness ratio are assumed to be $\beta = h/l = 1$ and $\alpha = t/l = 0.1$. (Online version in colour.)

previous section. Using the mathematical requirement of eigenbuckling from equation (3.17) and combining with the expression of the non-dimensional axial force in equation (4.2), we have

$$\left(\frac{\sigma_1}{E\alpha^3}\right) 12(\beta + \sin\theta)\cos\theta = n^2\pi^2$$
$$\text{or } \tilde{\sigma}_{1_{\text{crit},n}} = \left(\frac{\sigma_1}{E\alpha^3}\right)_{\text{crit},n} = \frac{n^2\pi^2}{12(\beta + \sin\theta)\cos\theta}, \quad n = 1, 2, 3\cdots \tag{4.4}$$

Here, $\tilde{\sigma}_{1_{\text{crit},n}}$ is the critical buckling stress ratio for direction 1 for different values of n. This is a key result in the paper as it gives a simple and exact closed-form expression of the critical

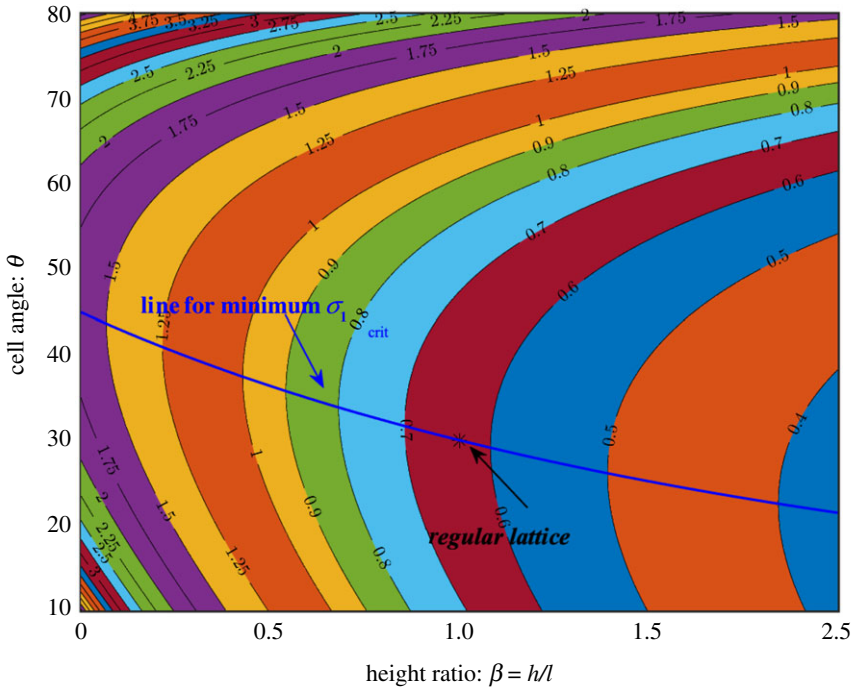

Figure 4. Contours of the normalized critical buckling stress $\sigma_{1_{crit}}/E\alpha^3$ plotted as a function of the cell angle θ and the height ratio $\beta = h/l$. The critical buckling stress is the minimum value when $2\sin^2\theta + \beta\sin\theta = 1$. This line is shown along with a mark denoting the regular lattice (that is, $\theta = \pi/6$ and $\beta = 1$). (Online version in colour.)

eigenbuckling stress for a general hexagonal lattice. Different values of n in equation (4.4) give different buckling modes. Higher values of n will lead to complex buckling mode shapes with mire ripples. To obtain the minimum value of the critical buckling stress, $n = 1$ needs to be selected. This minimum critical eigenbuckling stress will be denoted by $\tilde{\sigma}_{1_{crit}}$. We note that $\tilde{\sigma}_{1_{crit}}$ is purely a function of geometric parameters only. Values obtained from this formula are marked with a '*' in figure 3. They match with the numerical results as the expression is exact. The thickness ratio $\alpha = t/l$ appears in a cubic power. This implies that lattices with thicker elements will have a considerable higher critical buckling stress.

In figure 4, we show the contours of the normalized critical buckling stress $\sigma_{1_{crit}}/E\alpha^3$ as a function of the cell angle θ and the height ratio $\beta = h/l$. This is a general representation, and it is applicable for any hexagonal lattice. The actual critical buckling stress can be obtained directly by multiplying the values in figure 4 with $E\alpha^3$. For the special case of a regular lattice, we have $\theta = \pi/6$ and $\beta = h/l = 1$. Substituting these in equation (4.4), one obtains

$$\tilde{\sigma}_{1_{crit}} = E\frac{\pi^2\alpha^3}{9\sqrt{3}} \quad \text{or } \sigma_{1_{crit}}|_{\text{regular}} \approx 0.63E\left(\frac{t}{l}\right)^3. \tag{4.5}$$

This value is marked by the asterisk (*) in figure 4.

From equation (4.4), we observe that the critical buckling stress ratio $\tilde{\sigma}_{1_{crit}}$ depends on two parameters, namely β and θ. As seen from figure 4, the dependence on θ and β is not monotonic in nature. It is of practical engineering interest to find the minimum value of $\sigma_{1_{crit}}$ as θ and β change. Differentiating the expression in equation (4.4) with respect θ and equating it to zero, we obtain the condition for minimum $\tilde{\sigma}_{1_{crit}}$ as

$$\frac{\partial\tilde{\sigma}_{1_{crit}}}{\partial\theta} = 0 \implies 2\sin^2\theta + \beta\sin\theta - 1 = 0. \tag{4.6}$$

Solving this equation, we obtain

$$\theta = \sin^{-1}\left(\frac{\sqrt{\beta^2+8}-\beta}{4}\right) \quad \text{or } \beta = \frac{1-2\sin^2\theta}{\sin\theta}. \tag{4.7}$$

Depending on whether θ or β is known, the above expressions can be used to obtain the other parameter which will lead to the minimum critical buckling stress. The line represented by this equation is shown in figure 4. It can be observed that the combination of θ and β represented by this line will result in the minimum critical buckling stress. For engineering design considerations, such values may be avoided to achieve higher critical buckling stress. Alternatively, if stress-induced softening behaviour to be exploited in lattice metamaterials, then parameter combination in equation (4.7) must be selected for efficiency.

5. Eigenbuckling in the transverse direction

In figure 5, we show the hexagonal lattice subjected to compressive stress in the transverse direction. In the same figure, forcing on the unit cell due to this applied stress is also shown. It can be observed that the compressive axial force in the inclined beam is $N = W\sin\theta$, where

$$W = \sigma_2 bl\cos\theta. \tag{5.1}$$

Here, σ_2 is the applied stress and b is the out-of-plane thickness of the lattice. Using these, the non-dimensional axial force appearing in equation (2.10) can be obtained as

$$\begin{aligned} \mu^2 &= \frac{Nl^2}{EI} = \frac{\sigma_2 bl\sin\theta\cos\theta l^2}{Ebt^3/12} = \left(\frac{\sigma_2}{E\alpha^3}\right)12\sin\theta\cos\theta \\ \text{or } \mu &= \sqrt{\left(\frac{\sigma_2}{E\alpha^3}\right)12\sin\theta\cos\theta}. \end{aligned} \tag{5.2}$$

Substituting d_1 from equation (2.11) in equation (2.4), we can express the Young's modulus explicitly in terms of the above non-dimensional axial force parameter as

$$E_2 = \frac{E\alpha^3\mu^3\sin(\mu)(\beta+\sin\theta)}{\mu^3\sin(\mu)\alpha^2(2\beta+1)\cos\theta - (\mu^3\sin(\mu)\alpha^2+12\Delta)\cos^3\theta}. \tag{5.3}$$

This is the explicit expression of the equivalent elastic modulus E_2 of hexagonal lattices subjected to compressive stress as in figure 5.

Substitution of μ from equation (5.2) in the expression of E_2 in equation (5.3) shows that the Young's modulus E_2 is depended on the applied stress σ_2. This is a nonlinear behaviour, as observed before in the previous section. The ratio $\sigma_2/E\alpha^3$ is a non-dimensional quantity quantifying the applied compressive stress in direction 2 relative to Young's modulus of the constitutive material. In figure 6, variation of the effective Young's modulus E_2 with respect the relative compressive stress $\sigma_2/E\alpha^3$ is shown. The y-axis is normalized with $E\alpha^3$ as the x-axis. Results for four values of the cell angle θ are shown and the height ratio and thickness ratio are considered to be $\beta = h/l = 1$ and $\alpha = t/l = 0.1$. As the applied compressive stress increases, the effective Young's modulus E_2 reduces. As before, this is expected as the axial compression results in a loss of stiffness in the constituent beams. The stable and unstable (buckled) regions are marked in figure 6 based on whether $E_1 > 0$ or not.

Using the mathematical requirement of eigenbuckling from equation (3.17) and combining with the expression of the non-dimensional axial force in equation (5.2), we have

$$\begin{aligned} \left(\frac{\sigma_2}{E\alpha^3}\right)12\sin\theta\cos\theta &= n^2\pi^2 \\ \text{or } \tilde{\sigma}_{2_{\text{crit},n}} = \left(\frac{\sigma_2}{E\alpha^3}\right)_{\text{crit},n} &= \frac{n^2\pi^2}{12\sin\theta\cos\theta}, \quad n = 1,2,3\cdots \end{aligned} \tag{5.4}$$

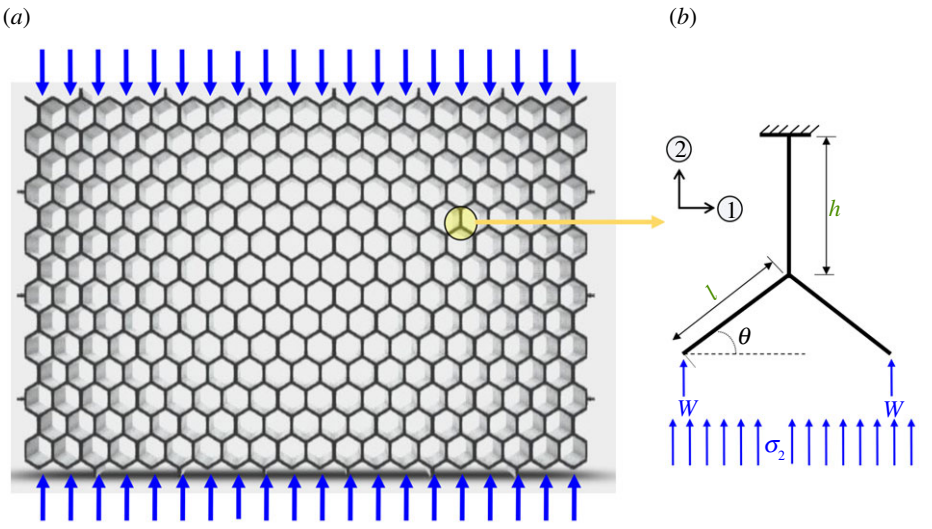

Figure 5. (*a*) Hexagonal lattice subjected to compressive stress σ_2 in the 2-direction. (*b*) Forcing in the constituent beams within the unit cell model. The compressive axial force is $W \sin\theta$ with $W = \sigma_2 bl \cos\theta$, where b is the out-of-plane thickness of the lattice. (Online version in colour.)

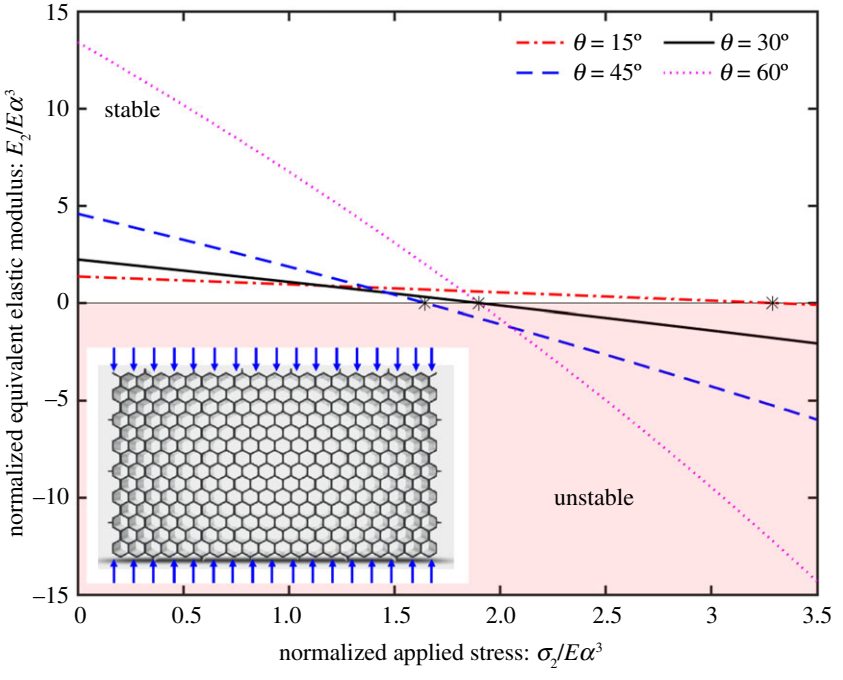

Figure 6. Variation of the effective Young's modulus E_2 with respect to the relative compressive stress in the 2-direction. The horizontal and vertical axis are normalized at $E\alpha^3$. Results for four values of the cell angle θ are shown. The values of the height ratio and the thickness ratio are assumed to be $\beta = h/l = 1$ and $\alpha = t/l = 0.1$. (Online version in colour.)

Here, $\tilde{\sigma}_{2_{\text{crit},n}}$ is the critical buckling stress ratio for direction 2. The minimum value of the critical buckling stress occurs for $n = 1$, and this minimum critical buckling stress is denoted by $\tilde{\sigma}_{2_{\text{crit}}}$. Values obtained from the formula (5.4) with $n = 1$ are marked with a '*' in figure 6, and they

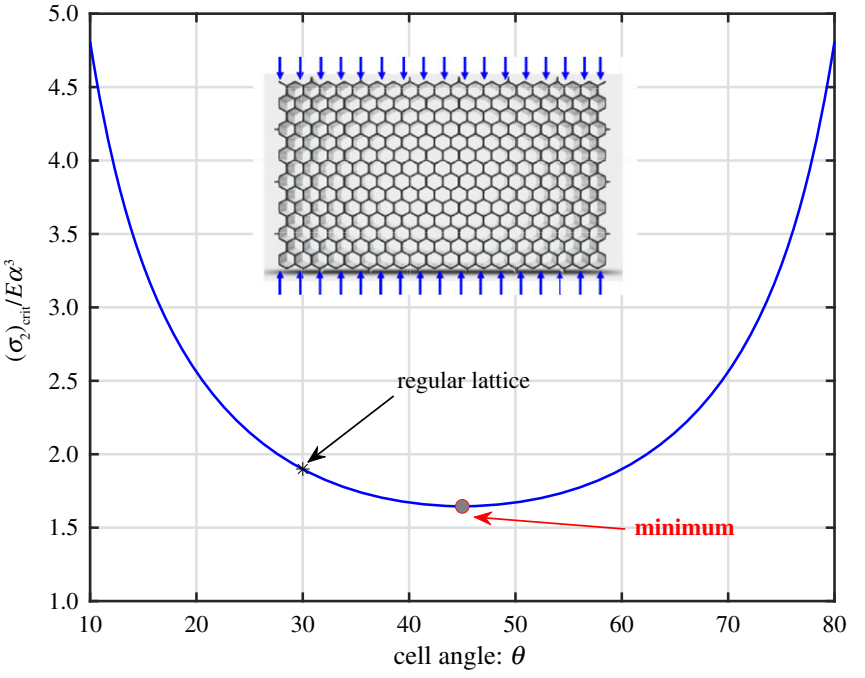

Figure 7. Normalized critical buckling stress $\sigma_{2_{crit}}/E\alpha^3$ plotted as a function of the cell angle θ. The minimum value occurs at $\theta = \pi/4$. This point is shown along with a mark denoting the regular lattice (that is, $\theta = \pi/6$ and $\beta = 1$). (Online version in colour.)

match with the numerical results for all the four values of θ shown in the plot. We again observe that $\tilde{\sigma}_{2_{crit}}$ is purely a function of the geometric parameters only.

In figure 7, we show the normalized critical buckling stress $\sigma_{2_{crit}}/E\alpha^3$ as a function of the cell angle θ. This is a generic representation, and it is applicable for any hexagonal lattice. The actual critical buckling stress can be obtained directly by multiplying the values in figure 7 with $E\alpha^3$.

For the special case of a regular lattice, using $\theta = \pi/6$ in equation (5.4), we have

$$\tilde{\sigma}_{2_{crit}} = E\frac{\pi^2\alpha^3}{3\sqrt{3}} \quad \text{or } \sigma_{2_{crit}}|_{regular} \approx 1.89E\left(\frac{t}{l}\right)^3 \approx 3\sigma_{1_{crit}}|_{regular}. \tag{5.5}$$

This value is marked by '*' in figure 7. The main difference between $\tilde{\sigma}_{1_{crit}}$ and $\tilde{\sigma}_{2_{crit}}$ is that the later does not depend on β. Differentiating the expression in equation (5.4) with respect to θ and setting it to zero, we obtain the condition for minimum $\tilde{\sigma}_{2_{crit}}$ as $\theta = \pi/4$. This value of the cell angle will result in the minimum buckling stress irrespective of the other geometric parameters of the lattice. For this value of θ, the minimum critical buckling stress becomes

$$\tilde{\sigma}_{2_{crit}}|_{min} = E\frac{\pi^2\alpha^3}{6} \quad \text{or } \sigma_{2_{crit}}|_{min} \approx 1.65E\left(\frac{t}{l}\right)^3. \tag{5.6}$$

This value is marked in figure 7 by a circle. Engineering designs can be checked against this value for safety.

6. Eigenbuckling due to stresses in both directions

In figure 8, we show the hexagonal lattice subjected to compressive stresses applied simultaneously in both directions. In the same figure, forces on the unit cell due to these applied stresses are also shown. This condition of applied stresses is also known as biaxial stress. The loading conditions discussed in the previous two sections can be viewed as special cases when

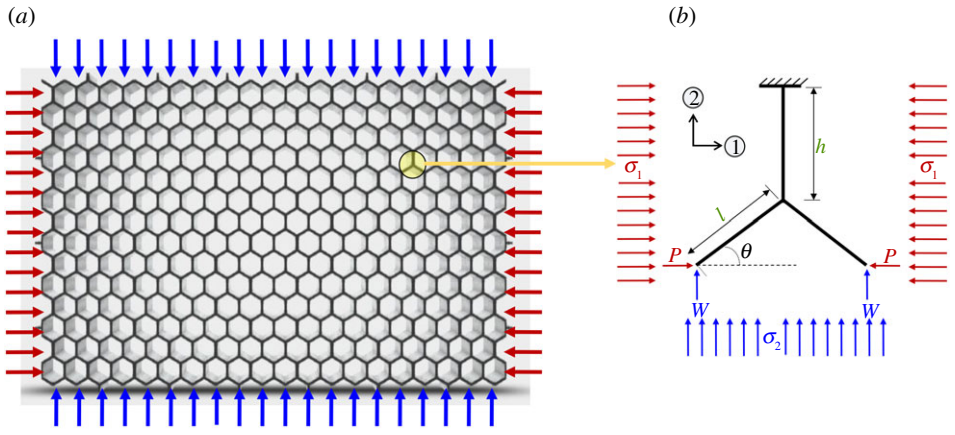

Figure 8. (*a*) Hexagonal lattice subjected to compressive stress in both 1 and 2-directions. Applied stresses in the two directions are σ_1 and σ_2 respectively. (*b*) Forcing in the constituent beams within the unit cell model. The compressive axial force is $P\cos\theta + W\sin\theta$ with $P = \sigma_1 b(h + l\sin\theta)$ and $W = \sigma_2 bl\cos\theta$, where b is the out-of-plane thickness of the lattice. (Online version in colour.)

forcing in one directions is considered to be zero. The axial force N within the individual beams are now functions of both σ_1 and σ_2. From figure 8*b*, we obtain the total axial forces as

$$N = P\cos\theta + W\sin\theta = \sigma_1 b(h + l\sin\theta)\cos\theta + \sigma_2 bl\sin\theta\cos\theta. \tag{6.1}$$

This is now coupled due to the fact that the axial force N within the individual beams is now a function of both σ_1 and σ_2. The non-dimensional axial force parameter can be obtained as

$$\mu^2 = \frac{Nl^2}{EI} = \frac{\sigma_1 b(h + l\sin\theta)\cos\theta l^2 + \sigma_2 bl\sin\theta\cos\theta l^2}{Ebt^3/12} \tag{6.2}$$

or

$$\mu = \sqrt{\left(\frac{\sigma_1}{E\alpha^3}\right)12(\beta + \sin\theta)\cos\theta + \left(\frac{\sigma_2}{E\alpha^3}\right)12\sin\theta\cos\theta}. \tag{6.3}$$

This expression of μ can be substituted in the analytical expressions of E_1 and E_2 given by equations (4.3) and (5.3) to obtain the effective elastic moduli when compressive stresses are applied in both directions.

Using the mathematical requirement of buckling from equation (3.17) and combining with the expression of the non-dimensional axial force in equation (6.2), we have

$$\left(\frac{\sigma_1}{E\alpha^3}\right)_{\text{crit},n} 12(\beta + \sin\theta)\cos\theta + \left(\frac{\sigma_2}{E\alpha^3}\right)_{\text{crit},n} 12\sin\theta\cos\theta = n^2\pi^2. \tag{6.4}$$

Rearranging this equation, we conveniently express it as an equation of a straight line

$$\frac{(\sigma_1)_{\text{crit},n}/E\alpha^3}{\{n^2\pi^2/12(\beta + \sin\theta)\cos\theta\}} + \frac{(\sigma_2)_{\text{crit},n}/E\alpha^3}{\{n^2\pi^2/12\sin\theta\cos\theta\}} = 1, \quad n = 1, 2, 3, \ldots. \tag{6.5}$$

In the above, $(\bullet)_{\text{crit},n}$ denotes critical buckling stress for any value of n. The minimum critical buckling stress, which is practically most important is obtained for $n = 1$ will be denoted as $(\bullet)_{\text{crit}}$ as before. The critical buckling stress obtained from the above equation is general and it is applicable for all values of the geometrical parameters α, β, and θ. This is shown in figure 9 for four values of θ. When $(\sigma_1)_{\text{crit}}/E\alpha^3$ and $(\sigma_2)_{\text{crit}}/E\alpha^3$ are plotted in x- and y-axis respectively, the line in equation (6.5) intercepts them at $\pi^2/12(\beta + \sin\theta)\cos\theta$ and $\pi^2/12\sin\theta\cos\theta$. It is interesting to note that these are the exact values of the uniaxial critical buckling stresses obtained in the

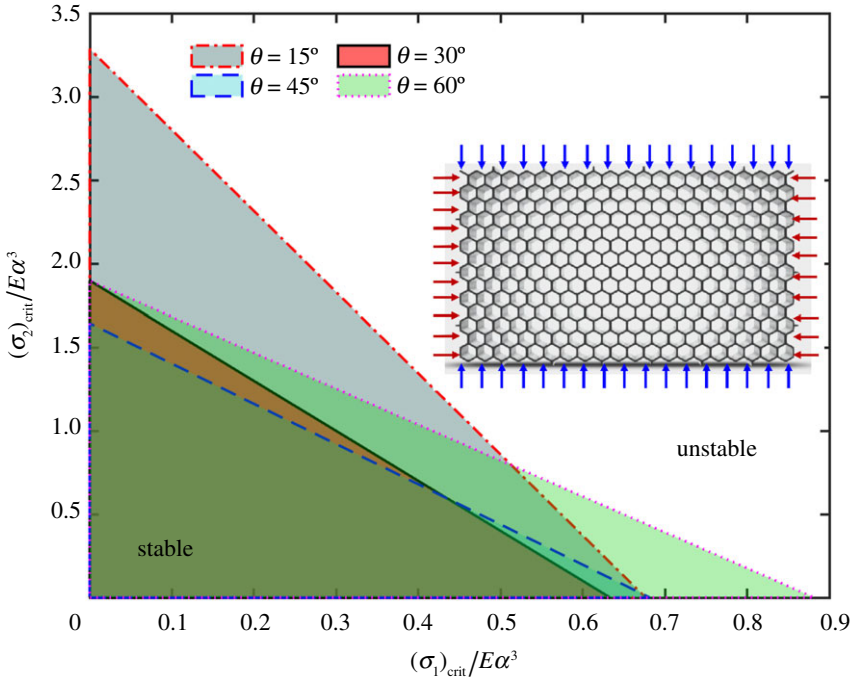

Figure 9. Biaxial critical stress for four values of the cell angle θ. The values of the height ratio and the thickness ratio are assumed to be $\beta = h/l = 1$ and $\alpha = t/l = 0.1$. The areas under the straight lines represent when the lattice is stable and the area outside the shaded region represents the buckled (unstable) state. (Online version in colour.)

previous two subsections. This implies that the biaxial case in equation (6.5) is the general case, and it degenerates to the specific uniaxial cases when the stress in the other direction becomes 0.

To obtain the minimum biaxial critical buckling stress, we minimize the area under the triangle in figure 9. The non-dimensional area is given by

$$A_s = \frac{1}{2}\left\{\frac{\pi^2}{12(\beta+\sin\theta)\cos\theta}\right\}\left\{\frac{\pi^2}{12\sin\theta\cos\theta}\right\}. \tag{6.6}$$

Differentiating this with respect θ and setting it to zero, we obtain the condition for minimum biaxial critical buckling stress as

$$\frac{\partial A_s}{\partial\theta} = 0 \implies 4\sin^3\theta + 3\beta\sin^2\theta - 2\sin\theta - \beta = 0. \tag{6.7}$$

This is a cubic equation in $\sin\theta$ and a linear equation in β. Solving this equation, we obtain

$$\theta = \sin^{-1}\left(\frac{\eta^{2/3} - 3\beta\sqrt[3]{\eta} + 9\beta^2 + 24}{12\sqrt[3]{\eta}}\right),\ \eta = 108\beta - 27\beta^3 + 12\sqrt{-81\beta^4 - 27\beta^2 - 96}$$
$$\text{or } \beta = \frac{2\sin\theta\left(2\sin^2\theta - 1\right)}{1 - 3\sin^2\theta}. \tag{6.8}$$

The cubic equation (6.8) is solved following the Cardano's formula used before (see equations (3.7)–(3.9)). Depending on whether θ or β is known, the above expressions can be used to obtain the other parameter which will lead to the minimum biaxial critical buckling stress. Numerical calculations using equation (6.8) show that for $0 \le \beta \le 2$, we have $45 \ge \theta \ge 35$. For engineering design, such values should be checked for safe design under biaxial buckling.

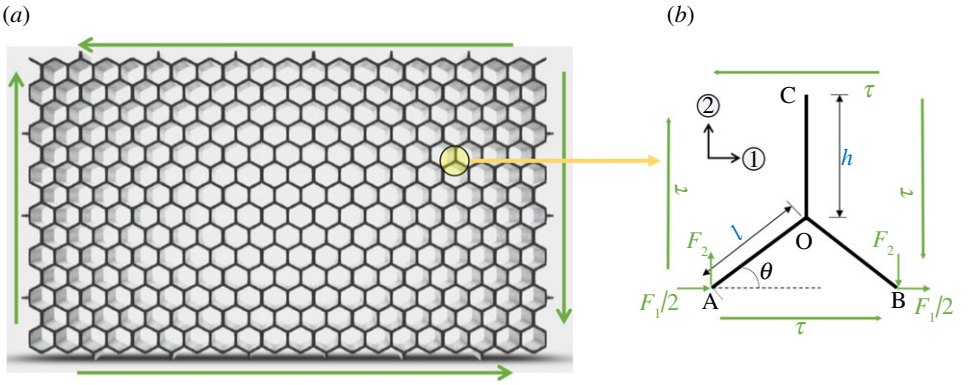

Figure 10. (*a*) Hexagonal lattice subjected to a torsional stress τ. (*b*) Forcing in the constituent beams within the unit cell model. The forces F_1 and F_2 are given by $F_1 = 2\tau lb\cos\theta$ and $F_2 = \tau b(h + l\sin\theta)$, where b is the out of plane thickness of the lattice. (Online version in colour.)

7. Eigenbuckling due to torsion

The hexagonal lattice subjected to a torsional stress τ is shown in figure 10. In the same figure, forcing on the unit cell due to this applied shear stress is also shown. It can be observed that the member AO is subjected to a compressive force while OB is subjected to a tensile force. As we are interested in buckling, the compressive force on AO is of primary interest. This can be obtained as

$$N = \frac{F_1}{2\cos\theta} + F_2\sin\theta = \tau lb\left(\cos^2\theta + (h/l + \sin\theta)\sin\theta\right) = \tau lb\,(1 + \beta\sin\theta)\,. \tag{7.1}$$

Here, τ is the applied shear stress and b is the out-of-plane thickness of the lattice. Using these, the non-dimensional axial force appearing in equation (2.10) can obtained as

$$\begin{aligned} \mu^2 &= \frac{Nl^2}{EI} = \frac{\tau lb\,(1 + \beta\sin\theta)\,l^2}{Ebt^3/12} = \left(\frac{\tau}{E\alpha^3}\right) 12\,(1 + \beta\sin\theta) \\ \text{or } \mu &= \sqrt{\left(\frac{\tau}{E\alpha^3}\right) 12\,(1 + \beta\sin\theta)}. \end{aligned} \tag{7.2}$$

Using the mathematical requirement of eigenbuckling from equation (3.17) and combining with the expression of the non-dimensional axial force in equation (7.2), we have

$$\begin{aligned} &\left(\frac{\tau}{E\alpha^3}\right) 12\,(1 + \beta\sin\theta) = n^2\pi^2 \\ \text{or } &\tilde{\tau}_{\text{crit},n} = \left(\frac{\tau}{E\alpha^3}\right)_{\text{crit},n} = \frac{n^2\pi^2}{12\,(1 + \beta\sin\theta)}, \quad n = 1, 2, 3, \ldots \end{aligned} \tag{7.3}$$

Here, $\tilde{\tau}_{\text{crit},n}$ is the critical torsional buckling stress ratio. The minimum value of the critical torsional buckling stress occurs for $n = 1$, and this minimum critical buckling stress is denoted by $\tilde{\tau}_{\text{crit}}$. We again observe that this is purely a function of the geometric parameters only.

In figure 11, we show the normalized critical torsional buckling stress $\tau_{\text{crit}}/E\alpha^3$ as a function of the cell angle θ and the height ratio $\beta = h/l$. For the special case of a regular lattice, using $\theta = \pi/6$ and $\beta = 1$ in equation (7.3), we have

$$\tilde{\tau}_{\text{crit}} = E\frac{\pi^2\alpha^3}{18} \quad \text{or } \tilde{\tau}_{\text{crit}}|_{\text{regular}} \approx 0.5483E\left(\frac{t}{l}\right)^3. \tag{7.4}$$

This value is marked by '*' in figure 11. Unlike the cases of axial stresses, there is no optimal combination of θ and β leading to the minimum value of the critical torsional buckling stress.

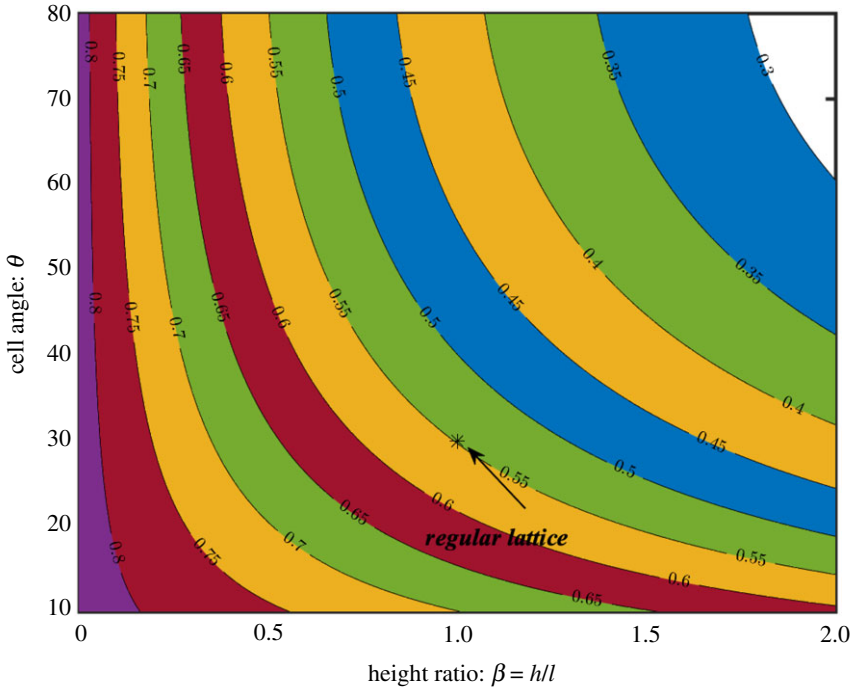

Figure 11. Contours of the normalized critical torsional buckling stress $\tau_{crit}/E\alpha^3$ plotted as a function of the cell angle θ and the height ratio $\beta = h/l$. The critical buckling stress corresponding to the regular lattice (that is, $\theta = \pi/6$ and $\beta = 1$) is marked in the figure. (Online version in colour.)

From equation (7.3), it can be observed that higher values of β will lead to lower critical torsional buckling stress values. This can be observed in figure 11 also.

8. Conclusion

The quantification of critical buckling stresses in cellular solids is of paramount importance. A physics-based analytical approach leading to closed-form expressions of critical in-plane buckling stresses in hexagonal elastic lattices was presented. The route to this analytical derivation is based on the spectral decomposition of the elasticity matrix of 2D materials. It was proved that the necessary and sufficient condition for buckling is that at least one eigenvalue of this matrix is zero. Following on from this condition, the third-order polynomial for the characteristic equation was solved exactly and the eigenvalues are obtained in closed form. This makes it possible to explicitly relate the eigenvalues with the equivalent elastic properties of the lattice material. The equivalent elastic properties are obtained considering a representative unit cell is composed of the Euler–Bernoulli beam element subjected to compressive axial force. They are expressed in terms of trigonometric functions of a non-dimensional axial force parameter. Through the axial force parameter, the eigenbuckling condition was linked to different applied stress conditions on the lattice. Four loading scenarios are considered, namely, when the stress is applied in the longitudinal direction only, when the stress is applied in the transverse direction only, when stresses are applied simultaneously in the longitudinal and transverse directions, and when a torsional stress is applied.

Using the condition of eigenbuckling, it was possible to solve the resulting nonlinear equations exactly in closed form to obtain the critical buckling stresses for axial torsional loading. The novel aspects of the proposed formulation include (1) explicit forcing parameter-dependent analytical expressions of the equivalent elastic constants appearing in the elasticity matrix, (2) exact solution

of the cubic characteristic equation arising from the eigenvalue problem involving the elasticity matrix, (3) establishing direct correspondences between the forcing parameter and different loading cases on the lattice and (4) quantifying the role of crucial non-dimensional geometric parameters on the critical buckling stresses. The main results can be expressed by the following general equations:

$$\sigma_{1_{\mathrm{crit},n}} = \frac{n^2\pi^2 E(t/l)^3}{12(h/l + \sin\theta)\cos\theta}, \quad \sigma_{2_{\mathrm{crit},n}} = \frac{n^2\pi^2 E(t/l)^3}{12\sin\theta\cos\theta}$$

and

$$\tau_{\mathrm{crit},n} = \frac{n^2\pi^2 E(t/l)^3}{12(1 + (h/l)\sin\theta)}, \quad n = 1, 2, 3, \ldots$$

Here, t is the thickness of the cell walls, θ is the cell angle, l and h are the lengths of the inclined and vertical elements of the hexagonal lattice. When compressive stresses are applied in both directions, a simple equation of a straight line was obtained. These expressions indicate that infinite number of eigenbuckling modes are possible. The effect of different geometric parameters of the lattice on the critical buckling stress has been explained graphically. One case is of particular practical interest is when the buckling stress is minimum. This has been investigated analytically and equations have been derived giving the critical parameter combinations for all the three axial loading conditions. For the longitudinal and transverse directions, the minimum critical eigenbuckling stress occurs when $h/l = (1 - 2\sin^2\theta)/\sin\theta$ and $\theta = \pi/4$, respectively. When compressive stresses are applied at both directions, the minimum critical eigenbuckling stress occurs for $h/l = 2\sin\theta(2\sin^2\theta - 1)/(1 - 3\sin^2\theta)$. Engineering design guidelines have been suggested based on these optimal eigenbuckling analyses. Future research may extend this work to investigate eigenbuckling of three-dimensional lattice materials considering spectral decomposition of the complete 6×6 elasticity tensor.

Data accessibility. This article has no additional data.

Competing interests. We declare we have no competing interests.

Funding. No funding has been received for this article.

Acknowledgements. The author gratefully acknowledges the financial support from the European Commission under the Marie Sklodowska Curie Actions (grant no. 799201-METACTIVE). Help from Ms M.F. Arago towards the finite-element results is highly acknowledged.

References

1. Christensen J, Kadic M, Kraft O, Wegener M. 2015 Vibrant times for mechanical metamaterials. *MRS Commun.* **5**, 453–462. (doi:10.1557/mrc.2015.51)
2. Zheng X. 2014 Ultralight, ultrastiff mechanical metamaterials. *Science* **344**, 1373–1377. (doi:10.1126/science.1252291)
3. Berger JB, Wadley HNG, McMeeking RM. 2017 Mechanical metamaterials at the theoretical limit of isotropic elastic stiffness. *Nature* **543**, 533–537. (doi:10.1038/nature21075)
4. Coulais C, Sounas D, Alù A. 2017 Static non-reciprocity in mechanical metamaterials. *Nature* **542**, 461–464. (doi:10.1038/nature21044)
5. Gibson L, Ashby MF. 1999 *Cellular solids structure and properties*. Cambridge: UK: Cambridge University Press.
6. Ongaro F. 2018 Estimation of the effective properties of two-dimensional cellular materials: a review. *Theor. Appl. Mech. Lett.* **8**, 209–230. (doi:10.1016/j.taml.2018.04.010)
7. Scarpa F, Adhikari S, Gil AJ, Remillat C. 2010 The bending of single layer graphene sheets: lattice versus continuum approach. *Nanotechnology* **20**, 085405. (doi:10.1088/0957-4484/21/12/125702)
8. Boldrin L, Scarpa F, Chowdhury R, Adhikari S, Ruzzene M. 2011 Effective mechanical properties of hexagonal boron nitride nanosheets. *Nanotechnology* **22**, 505 702:1–505 702:7. (doi:10.1088/0957-4484/22/50/505702)
9. Mukhopadhyay T, Mahata T, Adhikari S, Zaeem MA. 2017 Effective mechanical properties of multilayer nano-heterostructures. *Nat. Sci. Rep.* **7**, 158 181–158 18:13. (doi:10.1038/s41598-017-15664-3)

10. Singh A, Mukhopadhyay T, Adhikari S, Bhattacharya B. 2021 Equivalent in-plane voltage-dependent elastic moduli of piezoelectric 2D lattices. *Int. J. Solids Struct.* **208–209**, 31–48. (doi:10.1016/j.ijsolstr.2020.10.009)
11. Hohe JR, Becker W. 2002 Effective stress-strain relations for two-dimensional cellular sandwich cores: homogenization, material models, and properties. *Appl. Mech. Rev.* **55**, 61–87. (doi:10.1115/1.1425394)
12. El-Sayed FKA, Jones R, Burgess IW. 1979 A theoretical approach to the deformation of honeycomb based composite materials. *Composites* **10**, 209–214. (doi:10.1016/0010-4361(79)90021-1)
13. Zhang J, Ashby MF. 1992 The out-of-plane properties of honeycombs. *Int. J. Mech. Sci.* **34**, 475–489. (doi:10.1016/0020-7403(92)90013-7)
14. Mukhopadhyay T, Adhikari S. 2017 Effective in-plane elastic properties of quasi-random spatially irregular hexagonal lattices. *Int. J. Eng. Sci.* **119**, 142–179. (doi:10.1016/j.ijengsci.2017.06.004)
15. Zhang J, Ashby M. 1992 Buckling of honeycombs under in-plane biaxial stresses. *Int. J. Mech. Sci.* **34**, 491–509. (doi:10.1016/0020-7403(92)90014-8)
16. Triantafyllidis N, Schraad MW. 1998 Onset of failure in aluminum honeycombs under general in-plane loading. *J. Mech. Phys. Solids* **46**, 1089–1124. (doi:10.1016/S0022-5096(97)00060-4)
17. Klintworth J, Stronge W. 1988 Elasto-plastic yield limits and deformation laws for transversely crushed honeycombs. *Int. J. Mech. Sci.* **30**, 273–292. (doi:10.1016/0020-7403(88)90060-4)
18. Wang AJ, McDowell D. 2004 In-plane stiffness and yield strength of periodic metal honeycombs. *J. Eng. Mater. Technol.* **126**, 137–156. (doi:10.1115/1.1646165)
19. Cote F, Deshpande V, Fleck N, Evans A. 2004 The out-of-plane compressive behavior of metallic honeycombs. *Mater. Sci. Eng.: A* **380**, 272–280. (doi:10.1016/j.msea.2004.03.051)
20. Li K, Gao XL, Wang J. 2007 Dynamic crushing behavior of honeycomb structures with irregular cell shapes and non-uniform cell wall thickness. *Int. J. Solids Struct.* **44**, 5003–5026. (doi:10.1016/j.ijsolstr.2006.12.017)
21. Liu W, Wang N, Huang J, Zhong H. 2014 The effect of irregularity, residual convex units and stresses on the effective mechanical properties of 2D auxetic cellular structure. *Mater. Sci. Eng.: A* **609**, 26–33. (doi:10.1016/j.msea.2014.04.090)
22. Ruan D, Lu G, Wang B, Yu T. 2003 In-plane dynamic crushing of honeycombs? A finite element study. *Int. J. Impact Eng.* **28**, 161–182. (doi:10.1016/S0734-743X(02)00056-8)
23. Zheng Z, Yu J, Li J. 2005 Dynamic crushing of 2D cellular structures: a finite element study. *Int. J. Impact Eng.* **32**, 650–664. (doi:10.1016/j.ijimpeng.2005.05.007)
24. Yang MY, Huang JS. 2005 Elastic buckling of regular hexagonal honeycombs with plateau borders under biaxial compression. *Compos. Struct.* **71**, 229–237. (doi:10.1016/j.compstruct.2004.10.014)
25. Fan H, Jin F, Fang D. 2009 Uniaxial local buckling strength of periodic lattice composites. *Mater. Des.* **30**, 4136–4145. (doi:10.1016/j.matdes.2009.04.034)
26. Chen Q, Pugno NM. 2012 In-plane elastic buckling of hierarchical honeycomb materials. *Eur. J. Mech.-A/Solids* **34**, 120–129. (doi:10.1016/j.euromechsol.2011.12.003)
27. Haghpanah B, Papadopoulos J, Mousanezhad D, Nayeb-Hashemi H, Vaziri A. 2014 Buckling of regular, chiral and hierarchical honeycombs under a general macroscopic stress state. *Proc. R. Soc. A: Math., Phys. Eng. Sci.* **470**, 20130856. (doi:10.1098/rspa.2013.0856)
28. Mehrabadi MM, Cowin SC. 1990 Eigentensors of linear anisotropic elastic materials. *Q. J. Mech. Appl. Math.* **43**, 15–41. (doi:10.1093/qjmam/43.1.15)
29. Sutcliffe S. 1992 Spectral decomposition of the elasticity tensor. *J. Appl. Mech.* **59**, 762–773. (doi:10.1115/1.2894040)
30. Rivello RM. 1969 *Theory and analysis of flight structures*, 1st edn. New York: McGraw-Hill.
31. Adhikari S, Mukhopadhyay T, Liu X. 2021 Broadband dynamic elastic moduli of honeycomb lattice materials: a generalized analytical approach. *Mech. Mater.* **157**, 103796. (doi:10.1016/j.mechmat.2021.103796)
32. Horn RA, Johnson CR. 1985 *Matrix analysis*. Cambridge, UK: Cambridge University Press.
33. Abramowitz M, Stegun IA. 1965 *Handbook of mathematical functions, with formulas, graphs, and mathematical tables*. New York, NY: Dover Publications, Inc.
34. Kadic M, Buckmann T, Stenger N, Thiel M, Wegener M. 2012 On the practicability of pentamode mechanical metamaterials. *Appl. Phys. Lett.* **100**, 191901. (doi:10.1063/1.4709436)